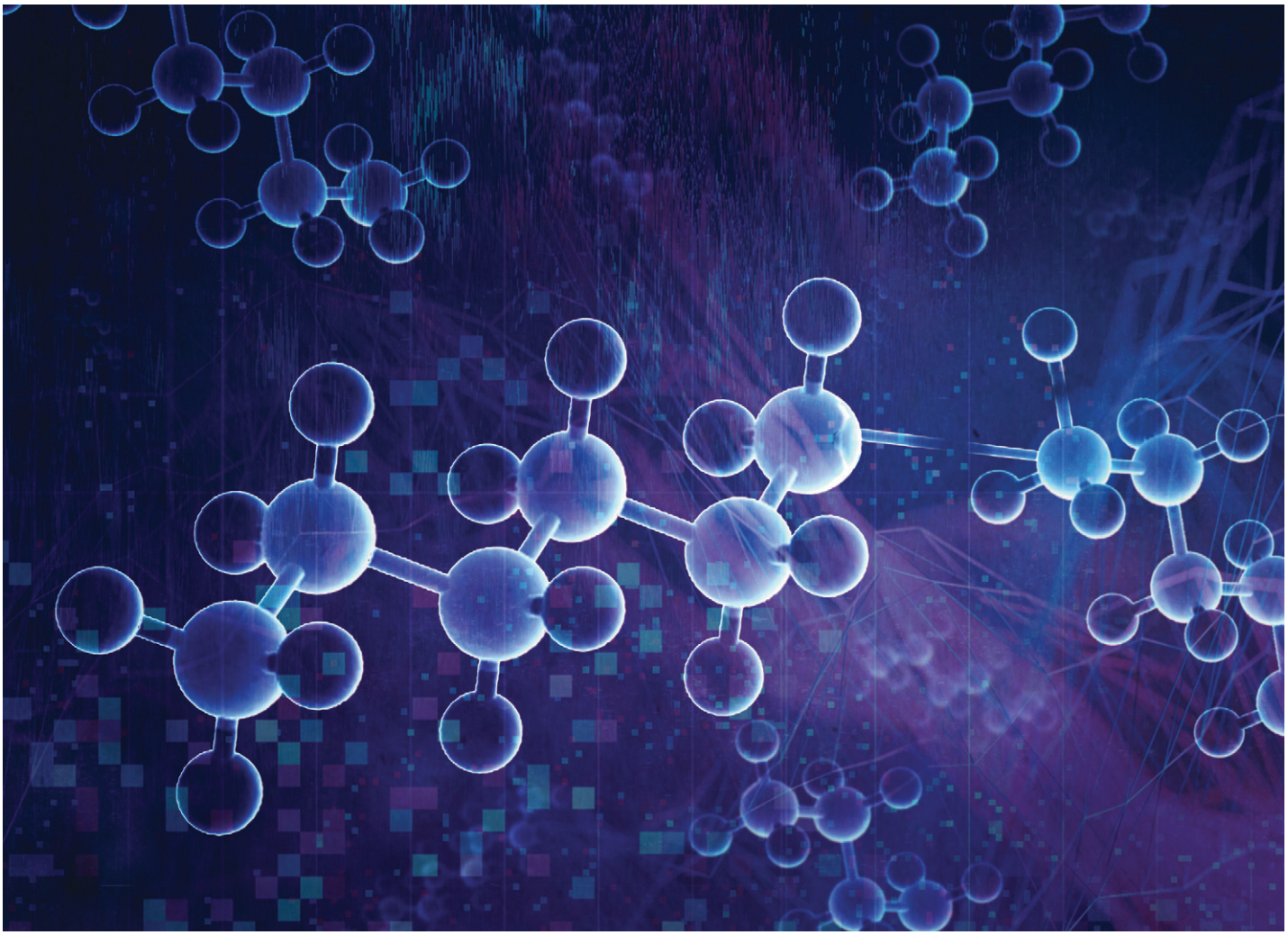

Showcasing research from Oliver Y. Gutiérrez, János Szanyi, and colleagues at the Pacific Northwest National Laboratory, USA.

Effect of reaction conditions on the hydrogenolysis of polypropylene and polyethylene into gas and liquid alkanes

Hydrogenolysis of polypropylene and polyethylene was studied as a pathway to smaller hydrocarbons. The work describes the impact of the polyolefin structure, reaction conditions, and presence of chlorine on the product distribution and branching degree.

As featured in:

See Oliver Y. Gutiérrez, János Szanyi *et al.*, *React. Chem. Eng.*, 2022, **7**, 844.

ROYAL SOCIETY OF CHEMISTRY

rsc.li/reaction-engineering

Registered charity number: 207890

Reaction Chemistry & Engineering

ROYAL SOCIETY OF CHEMISTRY

PAPER

View Article Online
View Journal | View Issue

Open Access Article. Published on 02 February 2022. Downloaded on 9/2/2025 8:32:14 PM.
This article is licensed under a Creative Commons Attribution-NonCommercial 3.0 Unported Licence.

Check for updates

Cite this: *React. Chem. Eng.*, 2022, 7, 844

Effect of reaction conditions on the hydrogenolysis of polypropylene and polyethylene into gas and liquid alkanes†

Linxiao Chen, ‡[a] Yifeng Zhu,‡[b] Laura C. Meyer, [a] Lillian V. Hale,[a] Thuy T. Le,[a] Abhi Karkamkar,[a] Johannes A. Lercher,[a] Oliver Y. Gutiérrez *[a] and János Szanyi *[a]

Received 30th September 2021,
Accepted 26th January 2022

DOI: 10.1039/d1re00431j

rsc.li/reaction-engineering

Hydrogenolysis of polypropylene (PP) and polyethylene (PE) provides a pathway to convert these plastics into smaller hydrocarbons at relatively low temperature. Among carbon (C)-supported transition metals, ruthenium (Ru) exhibited the highest efficacy, producing mixtures of C_1–C_{38} alkanes. The branching degree of the products depends on the position of the C–C cleavage, which can be tuned by the pressure of H_2. Liquid alkanes are produced below 225 °C and 200 °C from PP and PE, respectively, at 30 bar. The C distribution and branching level of the products remain invariant below full conversion of the initial polymer. Increasing H_2 pressure favors the hydrogenolysis of internal C–C bonds, reducing methane (CH_4) production, and favors linear over branched products. A liquid yield of >57% was achieved with PE under optimum conditions. We reveal the impact of the starting polyolefin structure, reaction conditions, and presence of chlorine on the product distribution and branching degree.

1. Introduction

The annual production of synthetic plastics totaled 367 million metric tons (Mt) in 2020, a nearly 200-fold increase compared to 1950.[1] Although this is still less than 5% of all petroleum and gas used in industry,[2,3] the use of plastic is foreseen to keep rising to the point of driving oil demand to 2050.[4] The concern associated with this trend is that most of the plastic being discarded accumulates in landfills and nature, posing severe threats to the environment.[5] Among the 6300 Mt plastic waste generated as of 2015, only 9% had been recycled, 12% was incinerated, and 79% was deposited in landfills.[6] As direct combustion is challenging, technologies that enable converting plastic waste into easily accessible energy carriers and other useful products ("upcycle") are needed.

The most common plastics are polyethylene (PE, 32 wt%) and polypropylene (PP, 23 wt%).[6] Currently, pyrolysis is the main approach to convert both compounds into smaller hydrocarbons.[7–9] Pyrolysis requires high reaction temperatures and provides low selectivity towards higher-value products. The cleavage of C–C bonds is also viable through hydrogenolysis; however, this approach is only beginning to be explored for polymer conversion.[10–13] Numerous recent reports are focusing on hydrogenolysis as a conversion strategy (Table 1 (ref. 14–24)). While several platinum (Pt)-group metals are being explored, Ru-based catalysts are attracting most of the attention from the research community.[19,20] Typically, the selectivity toward methane has been observed to decrease at high H_2 pressure.[20] Interestingly, while most studies are focusing on PE as the feedstock, the upcycling of PP, which has an even lower recycling rate than PE, has not been thoroughly explored or compared with PE.

Thus, information on how the polyolefin structure and specific composition (branching, impurities, and the presence of heteroatoms such as chlorine [Cl]) impact activity and selectivity of catalytic conversions is still lacking. These changing chemical and structural compositions are expected to have a very strong impact on the activity of potential metal catalysts, which requires the understanding of fundamental relationships between the catalyst nature and the (mixture) of reacting polymers. In this work we compare the hydrogenolysis of PE and PP on Ru, focusing on the influence of the polymer structure and H_2 pressure on product selectivity. We discuss the implications of our results in terms of the reaction mechanism and competitive adsorption of hydrogen, polymer, and alkane products over Ru catalysts.

We address these issues by targeting the hydrogenolytic conversion of PE and PP into liquid alkanes under relatively

[a] *Institute for Integrated Catalysis, Pacific Northwest National Laboratory, Richland, WA 99352, USA. E-mail: oliver.gutierrez@pnnl.gov, janos.szanyi@pnnl.gov*
[b] *Department of Chemistry, Fudan University, 200433, P.R. China*
† Electronic supplementary information (ESI) available. See DOI: 10.1039/d1re00431j
‡ These authors contributed equally.

This journal is © The Royal Society of Chemistry 2022

Open Access Article. Published on 02 February 2022. Downloaded on 9/2/2025 8:32:14 PM. This article is licensed under a Creative Commons Attribution-NonCommercial 3.0 Unported Licence.

Table 1 Recent progresses in the plastic upcycling by heterogeneous catalytic hydrogenolysis

Feedstock	Average M_w	Catalyst	T (°C)	Major products	Ref.
PE	~35 000	$Pt/SrTiO_3$	300	Alkanes	14
PE	~82 600	$mSiO_2/Pt/SiO_2$	250	Alkanes	15
PE	~3500	Pt/Al_2O_3	280	Alkylaromatics, alkylnaphthalenes (~C_{30})	16
PE	Not provided	Pt/C or SAPO	~25 (plasma)	Gaseous alkanes	17
PE	~120 000	$Pt–Re/SiO_2$	170	Low chain PE (M_w = 1300)	18
Aromatic polymers	Not provided	Ru/Nb_2O_5	200	Arenes	19
PE	~4000	Ru/C	200 to 250	Alkanes	20
PE	Not provided	Ru/C	220 to 280	Alkanes	21
PE	~4000 to ~50 000	Ru/CeO_2	240 to 300	Alkanes	22
PP	~12 000 and ~250 000	Ru/TiO_2	250	Alkanes	23
PP	~12 000 and ~340 000	Ru/C	200 to 250	Iso-alkanes	24
PE	~4000	Ru/C	150 to 250	Alkanes	This work
PP	~250 000				

mild conditions. We report the activity and selectivity for a series of supported metal catalysts, focusing in detail on the most active catalyst, Ru/C. The C_1–C_{38} products were analyzed in detail to establish the carbon distribution and branching level.

2. Experimental

2.1 Chemicals and pre-treatments

PP was purchased from Sigma-Aldrich (isotactic), with average M_w and M_n of ~250 000 g mol^{-1} and ~67 000, respectively. Before use, the large PP grains were crushed into small particles. PE also was purchased from Sigma-Aldrich as powder, with the average M_w and M_n of ~4000 g mol^{-1} and ~1300, respectively. The transition temperatures (T_g) of PP and PE are 160–165 °C and 106 °C, respectively. Ru/C, Rh/C, Pt/C, palladium (Pd)/C, iridium (Ir)/C, and nickel (Ni)/C at 5 wt% were purchased from Sigma-Aldrich. Prior to the reaction or transmission electron microscopy (TEM) measurements, the catalysts were pre-reduced in 5% H_2/nitrogen (N_2) flow at 200 °C for 3 h and then passivated in 1% O_2/N_2 flow. Ethyl acetate (EtOAc) for product extraction was also purchased from Sigma-Aldrich (high-pressure liquid chromatography grade, ≥99.8%).

2.2 Catalytic tests and post-reaction treatments

In a typical procedure, 100 mg of catalyst was mixed with 1000 mg PP/PE in a glass vial (3.7 mL, Fisherbrand). This mixture then was heated to melt the polymer and integrate the catalyst powder in it. The polymer–catalyst mixture then was placed into an autoclave reactor with a total internal volume of 125 mL. The reactor was sealed, and oxygen was removed by pressurizing with H_2 and venting in at least five successive cycles. Finally the reactor was pressurized with H_2 to the desired pressure, and then heated to the reaction temperature. Upon heating, the pressure increased but then remained relatively invariant during the reaction. We did not use any solvent, and we did not apply stirring. After the reaction, the reactor was quenched in an ice bath. The gas was collected by releasing the gas into a gas-sampling bag (Tedlar®) at room temperature and analyzed by gas chromatography-thermal conductivity detection (GC-TCD) (Inficon Micro GC Fusion gas analyzer with a four-module chassis). The liquids condensed inside the autoclave were dissolved with EtOAc and collected. The post-reaction solid composed of the catalyst and residual oligomers and polymers was further extracted with EtOAc. After filtration, the solution was combined with the liquids and analyzed by gas chromatography-mass spectroscopy (GC-MS) (Agilent 7890A GC, DB-5 column, Agilent 7693 autosampler and Agilent 5975C mass spectrometer) for identification and gas chromatography-flame ionization detection (GC-FID) (Agilent 7890A GC, DB-5 column, Agilent 7693 autosampler) for quantification. The solid residue was dried in an oven at 80 °C, weighed and the resulting mass was corrected for weight of catalyst added.

2.3 Product analysis

The solid residue after EtOAc extraction was completely dried and then weighed. The solid conversion, which is not the "polymer conversion", was calculated as:

$$\text{Solid conversion}\ (\%) = \frac{m_{\text{polyolefin}} - m_{\text{solid polymer residue}}}{m_{\text{polyolefin}}} \times 100$$

Liquid products (C_6–C_{38}) were quantified by GC-FID, with butyl-cyclohexane (Sigma-Aldrich, >99%) as the internal standard. The response factor for alkanes of each C number and the retention time of each *n*-alkanes were obtained with a C_7–C_{30} *n*-alkane standard (Supelco, 1000 μg mL^{-1} in *n*-hexane) and a C_{10}–C_{40} even *n*-alkane standard (Supelco, 50 μg mL^{-1} in *n*-heptane). The response factors in the concentration range of the product solution can be found in Table S2.† All peaks between *n*-C_kH_{2k+2} and *n*-$C_{k-1}H_{2k}$ were assumed as branched C_k alkanes unless GC-MS suggested otherwise. Although peaks from branched C_7 products and *n*-C_6H_{14} overlap with the large EtOAc peak, these products are of low concentration and evaporate to some extent during handling, so they only account for <1% of total C. Therefore, the inability to quantify such products does not affect our analysis nor the C balance in a meaningful way.

Open Access Article. Published on 02 February 2022. Downloaded on 9/2/2025 8:32:14 PM.
This article is licensed under a Creative Commons Attribution-NonCommercial 3.0 Unported Licence.

The gaseous products (C_1–C_5) were quantified using a micro-GC-TCD instrument (Inficon Micro GC Fusion gas analyzer) equipped with four columns (12 m Rt®-Q-Bond, 10 m Rxi®-1 ms, 10 m Rt®-Alumina BOND/Na_2SO_4 and 10 m Rt®-Msieve 5A). Before every analysis run the GC instrument was purged with N_2 followed by calibration with a calibrating gas mixture (Matheson) of N_2, H_2, carbon monoxide, carbon dioxide, methane, ethane, ethylene, propane, propylene, isobutane, *n*-butane, and *n*-butene. For the sample analysis, the gas sampling bag was connected to the GC and after flushing the sampling loop, the reaction gas mixture was measured several times until constant signals were obtained. The fraction of each alkane in the mixture was converted to its absolute quantity by the reactor volume (125 mL), and the post-reaction pressure was recorded at room temperature.

Because both PE and PP have high average M_W (4000 and 250 000 g mol^{-1}, respectively) and large average chain length (285 and 17 858 C units, respectively), the stoichiometry of C : H is close to 1 : 2, which allows us to calculated moles of C in the starting polymers based on their mass. With the information discussed above, the C yield of each phase was calculated as:

$$\text{C yield of solid, liquid, or gas (\%)} = \frac{\text{mol of C in solid, liquid, or gas}}{\text{mol of C in the starting polyolefin}} \times 100$$

The C selectivity of each phase was calculated as:

$$\text{C selectivity of solid, liquid, or gas (\%)} = \frac{\text{mol of C in solid, liquid, or gas}}{\text{mol of total quantified C}} \times 100$$

The C yield of each C number from C_1 to C_{38} was calculated as:

$$\text{C yield of } C_x\ (\%) = \frac{\text{mol of C in } C_x \text{ products}}{\text{mol of C in the starting polyolefin}} \times 100$$

2.4 Catalyst characterization

TEM measurements were performed on an FEI Tecnai F20 electron microscope to determine the metal particle size distribution on all C-supported catalysts. Each catalyst was ground and ultrasonically dispersed in ethanol. Drops of the suspension were applied on a copper grid coated with a carbon film and measurements were carried out with an electron detector with a 200 keV acceleration voltage. The elemental analysis was performed using an EDAX Si (Li) EDS detector and FEI TIA analysis software. Statistical analysis of the metal particle size was realized by counting >300 particles in several places of the mesh. The mean particle size was calculated using the following equation:

$$d_{TEM} = \frac{\sum n_i d_i^3}{\sum n_i d_i^2}$$

where d_{TEM} is the volume-area mean diameter of the particle, d_i is the diameter of the particle, measured from TEM images, and n_i is the number of particles with diameter d_i.

Inductive coupled plasma (ICP) was performed to determine Ru loading on Ru/C. The Ru/C catalyst was digested in concentrated nitric acid in a sealed microwave vessel. After the dissolution of all solids, the solution was analyzed on a Perkin Elmer Optima 7300DV ICP-OES instrument equipped with a cyclonic spray chamber and a Meinhard nebulizer.

H_2-Chemisorption was conducted with a Micromeritics ASAP 2020, in chemisorption mode, to determine Ru dispersion on Ru/C. Prior to the measurement, the catalyst was outgassed at room temperature, followed by reduction under H_2 at 523 K. The first adsorption isotherm was recorded at room temperature from 0.1 mbar to 600 mbar at 393 K. After evacuation at 393 K for 1 h, a second isotherm set was measured corresponding to physisorbed H_2 under the same conditions as the first isotherm. The concentration of chemisorbed H_2 was calculated by subtracting the two isotherms and extrapolating to zero H_2 pressure. A stoichiometry of 1 : 1 for metal : hydrogen was assumed to derive the dispersion from the concentration of chemisorbed hydrogen.

N_2-Physisorption was conducted to determine the specific surface area and pore volume of Ru/C on the same Micromeritics ASAP 2020 but in physisorption mode at liquid N_2 temperature (77 K). The sample was outgassed at 573 K for 2 h prior to the measurements. The textural properties were derived from the Brunauer–Emmett–Teller and Barrett–Joyner–Halenda models applied to the N_2 sorption data.

3. Results and discussion

3.1 Comparison of supported metals for polyolefin hydrogenolysis

A series of carbon-supported transition metals (*i.e.*, Ru/C, Rh/C, Pt/C, Pd/C, Ir/C, and Ni/C [all 5 at wt%]) was compared to establish the principal reactivity trend for converting PP and PE by hydrogenolysis (Table 2). Herein "gas products" refers to ≤C_5 alkanes, "liquid products" refers to EtOAc-soluble, GC-analyzable alkanes (*i.e.*, C_6–C_{38}, which are in the most desirable C range and not necessarily liquid at room temperature), and "solid products" refers to EtOAc-insoluble hydrocarbon oligomers or polymers. Unidentified products accounted for up to 35% of total C. For clarity, they are omitted in the following discussion, but their yield is described in the ESI.†

Table 2 shows the carbon yields of solid, liquid, and gas products on each catalyst after reaction for 18 h. Among the catalysts, Ru/C exhibited unique efficacy under the explored conditions, completely converting both PP and PE into gaseous products. Rh/C also produced gas and liquid products under these conditions but showed lower activity compared to Ru/C. While PE was completely converted with Rh/C into gases and liquids, 68% PP remained solid. For Pt/C, Pd/C, Ir/C, and Ni/C, the solid mass loss was <7%, with <1% combined gas and liquid yield, indicating low

 This journal is © The Royal Society of Chemistry 2022

Open Access Article. Published on 02 February 2022. Downloaded on 9/2/2025 8:32:14 PM.
This article is licensed under a Creative Commons Attribution-NonCommercial 3.0 Unported Licence.

Table 2 Comparing carbon-supported metal catalysts for the hydrogenolysis of polyolefins

Catalyst (5 wt%)	Metal particle size[a] (nm)	Carbon yield[b] (%) PP ($M_W \approx 250\,000$) Solid	Liquid	Gas	PE ($M_W \approx 4000$) Solid	Liquid	Gas
Blank	N/A	99.0	0	<0.1	96.4	0	0
Ru/C	2.4 ± 0.7	0	0	100	0	0	100
Rh/C	2.3 ± 0.7	68.2	6.4	5.7	0	35.1	17.3
Pt/C	2.4 ± 0.5	94.4	0	0.2	93.8	0	<0.1
Pd/C	2.8 ± 0.5	99.1	0	0.3	93.3	0	<0.1
Ir/C	2.8 ± 0.5	99.0	0	0.1	93.4	0	0.1
Ni/C	6 ± 1	99.4	0	<0.1	94.1	0	<0.1

[a] Derived from TEM (Fig. S1†) performed after reduction by H_2 at 250 °C and passivation by 1% O_2. [b] Reaction conditions: 250 °C, 30 bar H_2, 18 h, 1 g PP or PE, 100 mg catalyst.

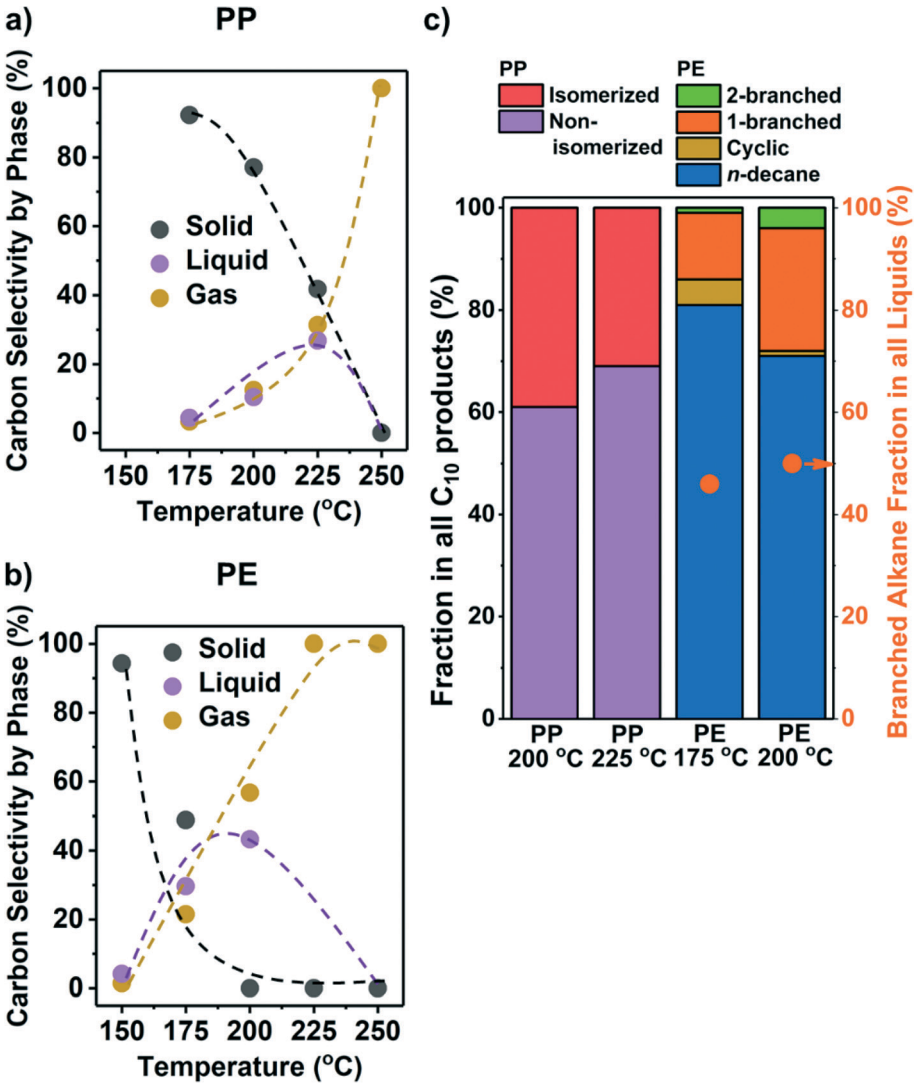

Fig. 1 Results from the hydrogenolysis of PP and PE at various temperatures. The C selectivity of solid (black), liquid (purple), and gas (yellow) among all identified C is shown in a) PP and b) PE (see Fig. S8a and b† for C yield including unidentified C, and Fig. S5† for C yield of C_1–C_{38} products by each carbon number). The distribution of C_{10} products at suitable temperatures for liquid production is shown in c) as stacked bars (see Fig. S4† for GC chromatograms and Table S3† for identities of the products). For PP, purple: non-isomerized alkanes (*i.e.*, 1–4 in Table S3†); red: isomerized alkanes; for PE, blue: *n*-decane; yellow: branched C_{10} cyclohexanes; orange: linear C_{10} alkanes with one branch; green: linear C_{10} alkanes with two branches. Orange dots in c) show the fraction of branched alkanes in all liquid (C_6–C_{38}) products for PE hydrogenolysis. Reaction conditions: 30 bar H_2, 18 h, 1 g PP or PE, 100 mg 5 wt% Ru/C.

Open Access Article. Published on 02 February 2022. Downloaded on 9/2/2025 8:32:14 PM.
This article is licensed under a Creative Commons Attribution-NonCommercial 3.0 Unported Licence.

hydrogenolysis activity under these conditions. Thermogravimetric analysis of fresh and spent Ru/C catalysts did not show signs of coke formation during the reaction.

The superior activity of Ru to other metals for alkane hydrogenolysis has been reported and attributed to the balanced coverage between chemisorbed hydrogen (*H) and chemisorbed hydrocarbon species ($*C_xH_y$).[20,25–28] The trend among the metals in Table 2 agrees well with the sequence of catalytic activity of metals reported by Rorrer *et al.* for *n*-octadecane, *i.e.*, Ru > Rh ≫ Ni/Pt.[20] It should be noted in passing that for C_2H_6 hydrogenolysis, the sequence was slightly different, *i.e.*, Ru > Rh/Ni/Ir ≫ Pt/Pd.[25,27] These differences are typical for hydrogenolysis of alkanes varying in size; that is, the structure sensitivity markedly decreases as the molecular size increases.[29,30]

3.2 Carbon distribution and branching level of liquid products

While the conversion on Ru/C (see Table S1 for ESI† characterization) at 250 °C failed to yield liquid products, lower temperatures improved the selectivity towards liquids (Fig. 1a and b). We repeated selected experiments and found that solid conversions and liquid/gas yields varied within 5% and 3%, respectively. Hydrogenolysis starts as low as 175 °C for PP and 150 °C for PE, with solid conversion increasing with temperature. We note that the lowest temperature (150 °C) at which Ru/C was found to convert PE is much lower than that of Pt catalysts reported in the literature (≥250 °C, Table 1). The conversion of PP requires higher temperature than PE suggesting that under our reaction conditions, PP is less reactive than PE. We cannot, however, discuss the reasons for such a difference because the polymers we investigated have many differences (*e.g.*, M_W, viscosity, chemical structure, *etc.*).

Liquid alkanes were only produced between 175 °C and 225 °C from PP and 150 °C and 200 °C from PE (Fig. 1a and b). Fig. S5† presents the C yield of C_1–C_{38} products (see Fig. S4† for examples of raw GC-FID data). The figures show that at appropriate temperatures, a mixture of liquid alkanes with wide distribution in molecular weight is produced from both polyolefins. The products of PE (Fig. S5b†) can be divided into the following three categories that are characteristic of the reacting substrate and the sequential processes occurring: 1) CH_4 from the hydrogenolysis of terminal C–C bonds, 2) *n*-alkanes from the hydrogenolysis of internal C–C bonds, and 3) branched alkanes from C–C cleavage at particular positions (see below). PP hydrogenolysis only yields CH_4 and branched alkanes without $>C_3$ *n*-alkanes, as the starting PP structure is highly methyl branched. Because CH_4 is a low-value product, it is desirable to steer the regioselectivity of hydrogenolysis towards internal C–C bonds. Isomerization may be desirable to increase the product branching level for higher fuel quality,[31] particularly with PE as the feedstock. Olefins or aromatics were not observed as products under the present conditions.

Branched alkanes accounted for ~50% of total C among all liquid products from PE (orange dots in Fig. 1c). All liquid products from PP were branched alkanes. The C_{10} products were analyzed in detail to gauge the branching level of liquid products and the location, where the C–C bonds are being cleaved. Fig. 1c shows that at temperatures leading to an appreciable liquid yield, products ranged from multiple branched alkanes from PP (Fig. S4b, Table S3†) to *n*-decane from PE, comprising >60% of total C_{10}. Most branched C_{10} alkanes from PE contain only one methyl or ethyl side chain (Fig. S4b, Table S3†). The relative absence of branched products with PE compared to PP indicates that metal-catalyzed isomerization is slow compared to C–C cleavage. The PP structure leads, in contrast, to a high degree of branching; the dominating C_{10} (80 wt%) products from PP hydrogenolysis were 2,4,6-trimethylheptane, 2,4-, 3,5-, and 2,6-dimethyloctane.

3.3 Effects of the reaction time on the product distribution

Let us in the next step establish the sequence of reactions as the conversion changes. Fig. 2a and b show that the conversion was completed in all cases at 36 h. Initially, the liquid and gas amounts produced increased monotonously with reaction time for PE and PP (see Fig. 2 and Table S4†). This indicates that liquid and gaseous alkanes were produced in parallel and that the net consumption of the liquid fraction only started after complete solid conversion (>24 h for PP and >36 h for PE). Fig. S6† shows that the C distribution in the liquid fraction did not change significantly before complete solid conversion (centered around C_{22} and C_{18} for PP and PE, respectively), and only started to shift towards shorter alkanes once the polymer was converted. This sequential reaction suggests that in the solvent free system the longer chains of the polyolefins were preferentially adsorbed, blocking secondary hydrogenolysis of intermediately formed hydrocarbons.

We attribute this effect to the large fraction of carbon atoms contained in the polymer chains. This must increase the probability of a fragment in the polymer, over small hydrocarbon molecules, to interact with the catalyst. Also, the size of such polymer fragments can be significantly larger than hydrocarbon molecules and therefore interact stronger with the catalyst. The dependence of the alkane adsorption energy, and hence hydrogenolysis rate, with chain length has been established with small alkanes and attributed to Van der Waals interactions with metal surfaces as well as entropic factors.[32,33]

Fig. 2c shows that for a fixed temperature and H_2 pressure the selectivity to CH_4 did not change until full conversion; that is, intermediately formed products are not able to access the metal surface in the presence of polymer. It should be noted in passing that the CH_4 selectivity at full conversion was expectedly higher with PP than with PE. It also should be noted that with incomplete conversion, the selectivity to branched alkanes from PE was constant allowing to estimate the degree of branching (*i.e.*, the products represent the primary cleavage from the polymer). Once the polymer was consumed, excess CH_4 and isomers formed. Overall, the results show conclusively

 This journal is © The Royal Society of Chemistry 2022

Open Access Article. Published on 02 February 2022. Downloaded on 9/2/2025 8:32:14 PM.
This article is licensed under a Creative Commons Attribution-NonCommercial 3.0 Unported Licence.

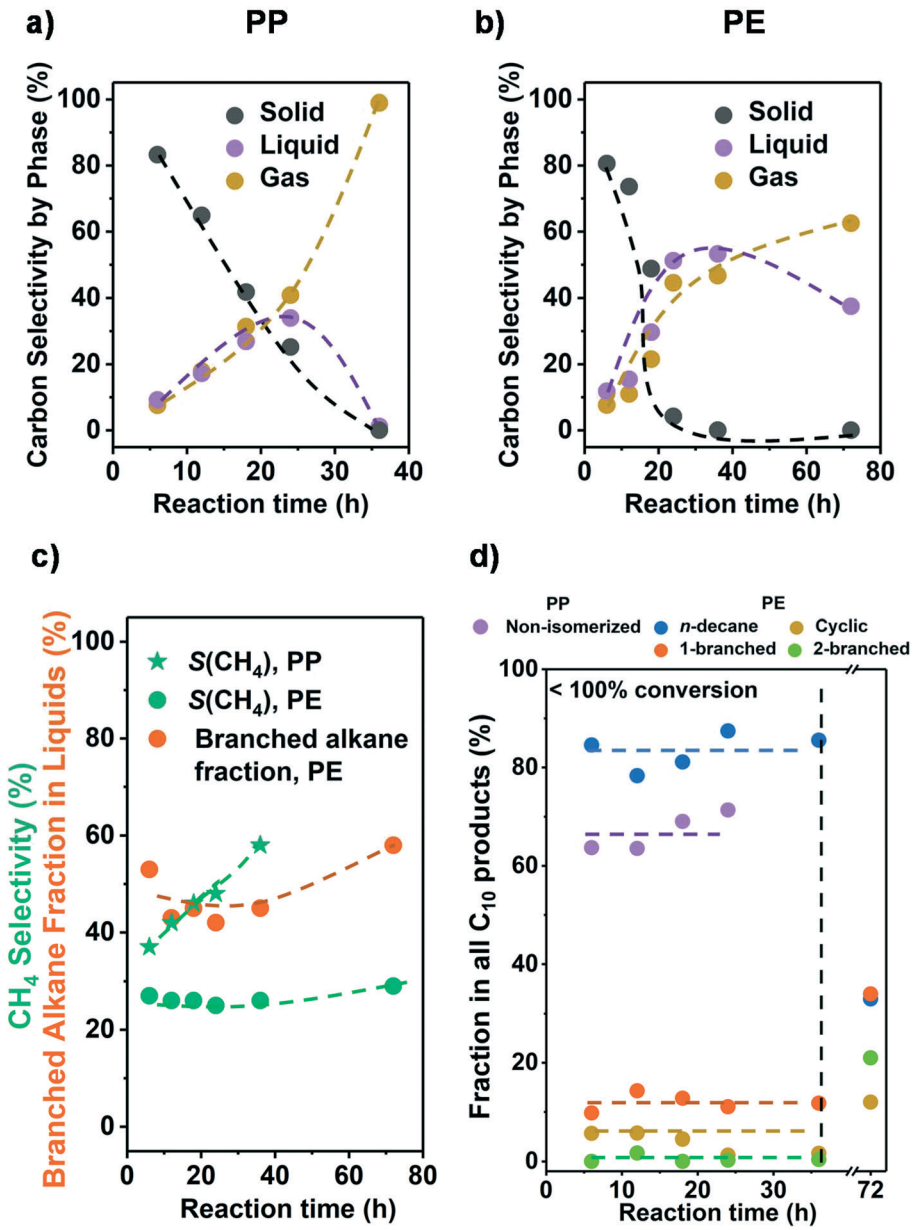

Fig. 2 Results from the hydrogenolysis of PP and PE for various time. The C selectivity of solid (black), liquid (purple), and gas (yellow) among all identified C is shown in a) PP and b) PE (see Fig. S7c and d† for C yield including unidentified C, and Fig. S6† for C yield of C_1–C_{38} products by each carbon number). The CH_4 selectivity and fraction of branched alkanes in all liquid products from PE are shown in c). The changes in C_{10} product distribution with time is shown in d) (for PP, purple: non-isomerized alkanes, *i.e.*, 1–4 in Table S3;† red: isomerized alkanes; for PE, blue: *n*-decane; yellow: branched C_{10} cyclohexanes; orange: linear C_{10} alkanes with 1 branch; green: linear C_{10} alkanes with 2 branches). Reaction conditions: 225 °C for PP and 175 °C for PE, 30 bar H_2, 1 g PP or PE, 100 mg 5 wt% Ru/C.

that it is possible to produce primary products as long as the product mixture is not exposed to the catalyst after complete conversion of the polymer.

3.4 Effects of the H_2 pressure on the reaction rate and selectivity

As the partial pressure of H_2 (P_{H_2}) has a profound impact on the hydrogenolysis of small alkanes,[25,27,34] we investigated its impact on conversion rates and selectivity (Fig. 3). For both polyolefins, the conversion was negligible without the presence of H_2 (*i.e.*, only traces of liquid products, mostly alkenes and cyclic alkanes were observed). For PP, the polymer conversion increased monotonously with P_{H_2} between 5 and 75 bar (Fig. 3a). For PE, however, conversion increased until P_{H_2} = 45 bar, and then decreased (Fig. 3b). We attribute this decrease to an excess of H_2 competing for binding and reaction sites. This is consistent with the hydrogenolysis of small alkanes, for which negative order in H_2 has been reported for transition metals including

Open Access Article. Published on 02 February 2022. Downloaded on 9/2/2025 8:32:14 PM.
This article is licensed under a Creative Commons Attribution-NonCommercial 3.0 Unported Licence.

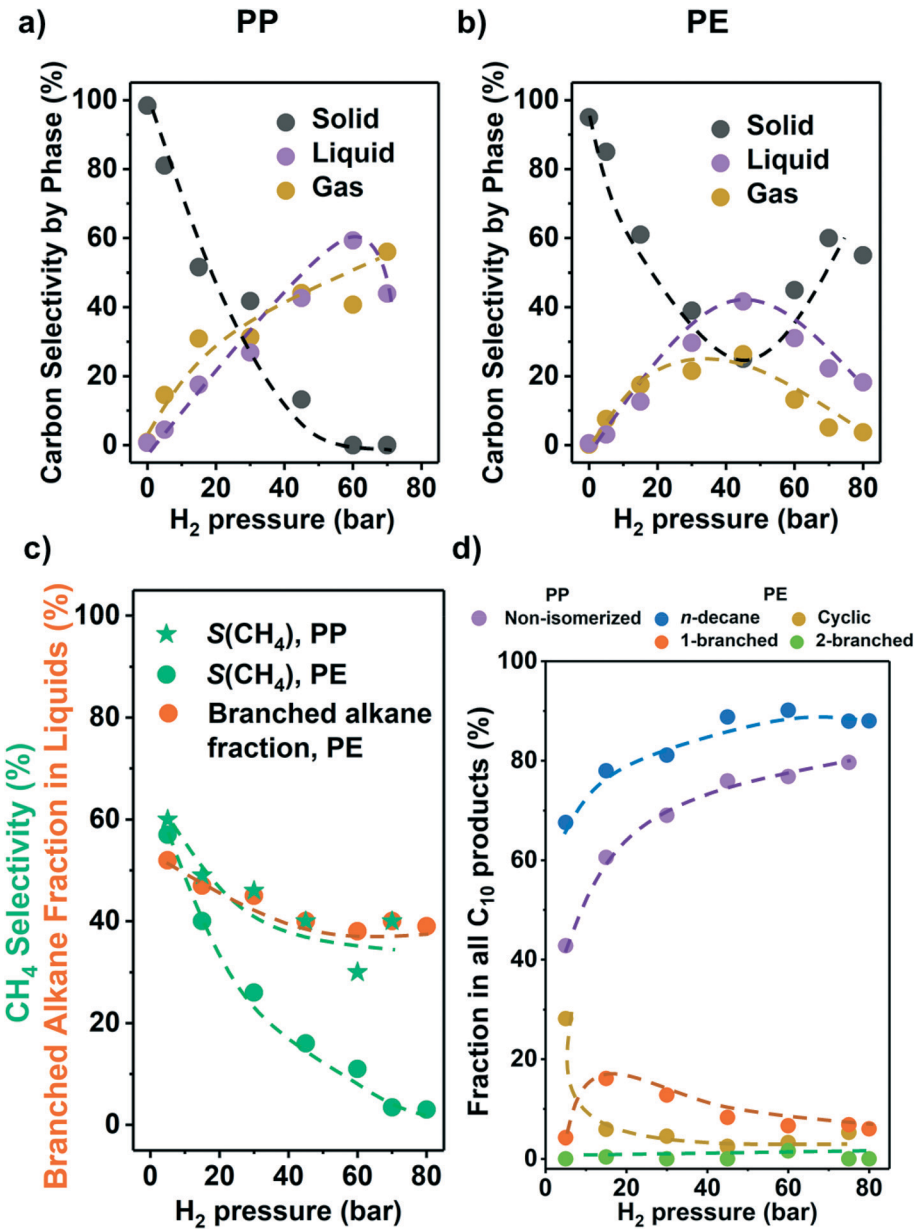

Fig. 3 Results from the hydrogenolysis of PP and PE under various H_2 pressure. The C selectivity of solid (black), liquid (purple), and gas (yellow) among all quantified C is shown in a) PP and b) PE (see Fig. S7e and f† for C yield including unidentified C, and Fig. S7† for C yield of C_1–C_{38} products by each carbon number). The CH_4 selectivity and fraction of branched alkanes in all liquid products from PE are shown in c). The changes in C_{10} product distribution with P_{H_2} is shown in d) (for PP, purple: non-isomerized alkanes, *i.e.*, 1–4 in Table S3;† red: isomerized alkanes; for PE, blue: *n*-decane; yellow: branched C_{10} cyclohexanes; orange: linear C_{10} alkanes with 1 branch; green: linear C_{10} alkanes with 2 branches). Reaction conditions: 225 °C for PP and 175 °C for PE, 18 h, 1 g PP or PE, 100 mg 5 wt% Ru/C.

Ru.[25,27,33,34] The subtle differences between PE and PP are attributed to the different reaction temperatures used for the two polymers, causing a lower H coverage with PP.

Fig. 3c shows that for both PP and PE, the CH_4 selectivity decreased with P_{H_2} below full conversion pointing to differences in the specific binding of the polymer branches with hydrogen pressure.[35] This decrease in CH_4 selectivity was concluded to be unrelated to varying conversion levels, because under constant P_{H_2}, the CH_4 selectivity was insensitive to conversion (Fig. 2c). It is interesting to note that that the CH_4 selectivity decreased monotonously with increasing P_{H_2} (Fig. 3c), even when the conversion was maintained constant. Thus, we conclude that increasing P_{H_2} leads to preferential hydrogenolysis of internal C–C bonds. We hypothesize that the strands of polymer are hindered to adopt the larger surface ensemble required for terminal C–C bond cleavage. More work to probe this hypothesis is, however, required. The maximum of the molecular weight distribution of the liquid products decreased with increasing P_{H_2} (Fig. S7†) for PP (*i.e.*, more light hydrocarbons being

 This journal is © The Royal Society of Chemistry 2022

Open Access Article. Published on 02 February 2022. Downloaded on 9/2/2025 8:32:14 PM.
This article is licensed under a Creative Commons Attribution-NonCommercial 3.0 Unported Licence.

formed). The fact that the maximum was nearly constant for PE suggests that the influence of adsorbed hydrogen is significantly more prominent for branched polymers.

At higher P_{H_2}, the fraction of branched alkanes in all liquid products from PE decreased (Fig. 3c), while the fraction of linear C_{10} in all C_{10} products from both polyolefins is higher (Fig. 3d). Also, at low P_{H_2} (5 bar), the fraction of cyclic C_{10} in all C_{10} products from PE increased significantly (yellow in Fig. 3d). Similar to the CH_4 selectivity, these trends in product branching and isomerization level are insensitive to the reaction time, or the solid conversion, under the same P_{H_2} (Fig. 2). Therefore, the changes in selectivity are not associated with the difference in the conversion level. Instead, the results indicate that higher P_{H_2} favors formation of linear products over branched ones.

Mechanistically, hydrogenolysis of the polymer strands on the metal surface occurs at dehydrogenated C–C units.[26,36–40] The dehydrogenation process weakens C–C bonds by formation of carbon–metal bonds, increasing the occupancy of antibonding orbitals in C–C bonds.[41,42] Intuitively, the formation of the corresponding dehydrogenated transition states requires multiple free adjacent metal sites to accommodate dissociated hydrogen. Therefore, this process is disfavored by relatively high H_2 pressures, at least at low reaction temperatures. An example for this is seen in the negative impact of high pressure on the conversion rate of PE at 175 °C.

Such mechanistic picture also helps explain our observations as shown in Fig. 4. For PP, the cleavage can occur between ^3C–^1C and ^3C–^2C bonds.

The cleavage of the former is kinetically favored (^3C–^1C is by far more abundant in PP) and ultimately leads to CH_4 upon hydrogenation of the resulting carbide. However, the formation of the corresponding transition states requires

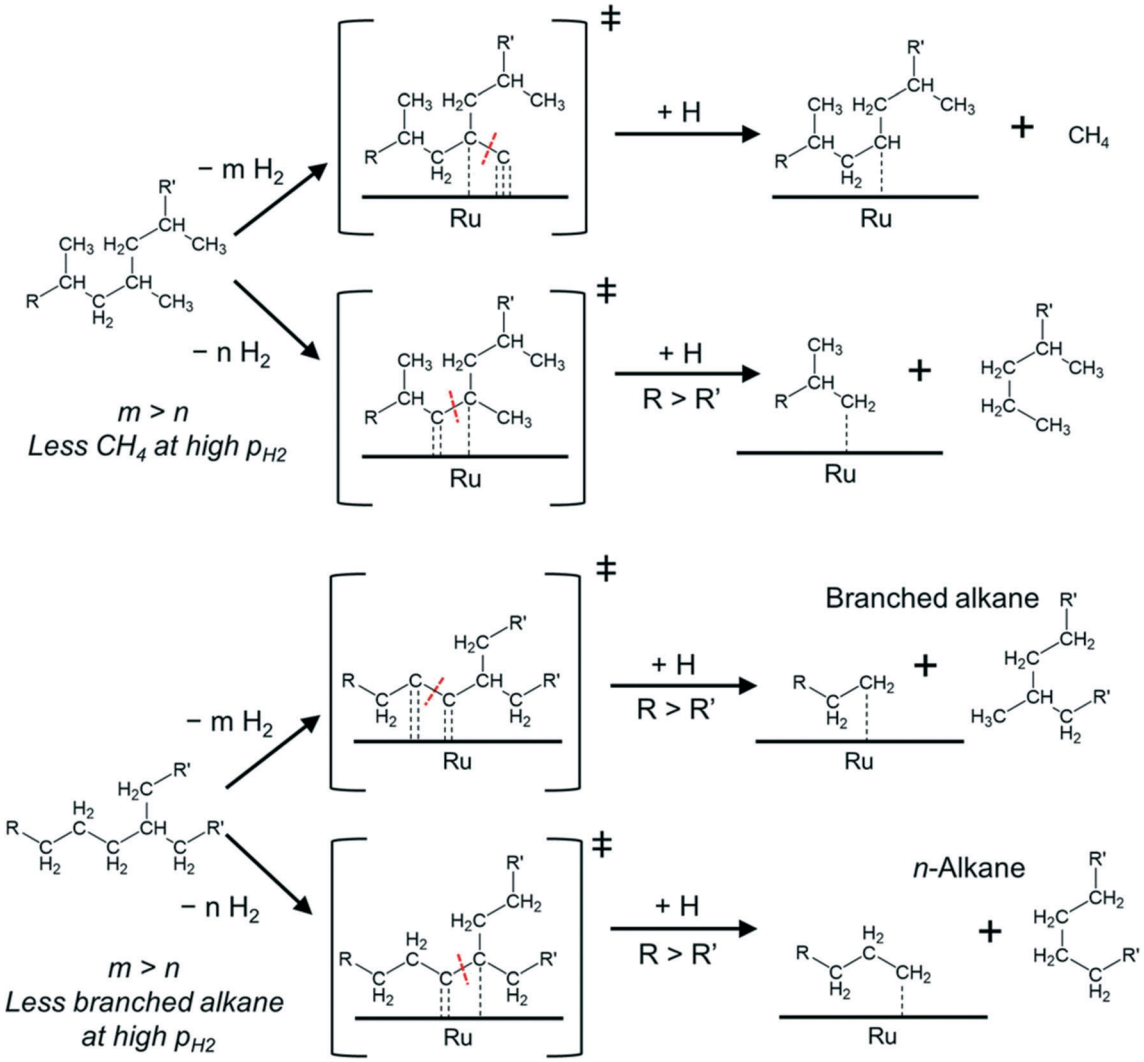

Fig. 4 Illustration of the proposed hydrogenolysis pathways for polypropylene (top) and polyethylene (bottom). The first steps of the reaction are adsorption and dehydrogenation, which lead to a hydrogen-depleted intermediate. Upon C–C cleavage, the hydrogenation of the fragments leads to the products. The lighter product (containing *R′* in the figure) will desorb preferentially, whereas the surface will remain covered with the longer hydrocarbon chains (the fragment containing *R* in the figure).

Open Access Article. Published on 02 February 2022. Downloaded on 9/2/2025 8:32:14 PM.
This article is licensed under a Creative Commons Attribution-NonCommercial 3.0 Unported Licence.

removing more hydrogen from the hydrocarbon chain than for the cleavage of a ^{3}C–^{2}C bond (which could lead to long alkane products). Thus, increasing P_{H_2}, and the concomitant increase in hydrogen coverage, favors cleavage at ^{3}C–^{2}C positions over ^{3}C–^{1}C. Repulsive interactions between methyl groups and hydrogen at the metal surface could also hinder the oxidative adsorption of ^{1}C with increasing P_{H_2}.[43]

In the case of PE (with one branch every 50–100 C atoms[44–46]) cleavage can occur between ^{2}C–^{2}C and ^{3}C–^{2}C bonds, in addition to the expected cleavage between ^{x}C–^{1}C bonds. If the cleavage occurs at ^{2}C–^{2}C positions, near ^{3}C atoms, subsequent hydrogenation can produce branched alkanes (Fig. 4). In contrast, ^{3}C–^{2}C cleavage has higher probability to produce linear products. We hypothesize that the ^{2}C–^{2}C cleavage requires deeper dehydrogenation than the ^{3}C–^{2}C cleavage. Therefore, increasing P_{H_2} decreases the selectivity to branched products.

Note that in all cases, upon cleavage, the longer and less branched polymer strands have a stronger driving force to remain adsorbed at the surface[32] to undergo further reaction. This can lead to multiple ^{x}C–^{1}C transition states (particularly for PP), which push the selectivity towards methane.

3.5 High liquid yield under optimal conditions and the effects of Cl

Results indicate that low reaction temperatures (and high P_{H_2}) are required to maximize liquid products on Ru/C. Thus, we converted PE at 175 °C and 82 bar H_2. Fig. 5 shows the C yield in the three phases and C distribution from C_1 to C_{38}. A large fraction of only preliminary identified products forms a part of the liquid phase, *i.e.*, they are EtOAc-soluble, but they have carbon numbers $>C_{38}$ and therefore beyond detection by GC (see Table S4, Fig. S9,† and related discussion). Hence, Fig. 5 likely underestimates the liquid yield. A high liquid yield of 57 mol. C%, mostly in the diesel range (C_{12}–C_{20}), was achieved after 76 h. As anticipated, the gas yield and CH_4 selectivity at 100% solid conversion were only ~10% and ~3%, respectively. Beyond full conversion (>48 h, Fig. 5b) the larger alkanes ($>C_{25}$) were converted to lighter products without much gas production. In contrast, with H_2 at 30 bar, a significant fraction of the liquid products was gasified under such conditions (Fig. 2a and b). For PP, it was more difficult to suppress the formation of CH_4. By applying high P_{H_2} (60 bar), a maximum of 47% liquid yield at full conversion was achieved but with 30% CH_4 selectivity (Fig. S8e, Table S4†).

A potential challenge faced by hydrogenolysis-based processes is the presence of Cl because PP/PE plastic waste is often mixed with polyvinyl chloride (PVC) even after separation. Experiments in the presence of PVC showed release of HCl above 175 °C in the presence and absence of PP/PE with a strong detrimental effect on catalyst activity. Even at 0.1 wt% PVC (Table S5†), the unconverted fraction of PP increased from 27.6% without PVC, to 87.7%, and further to 96.7% with 1 wt% PVC (225 °C, 30 bar H_2). For PE, the

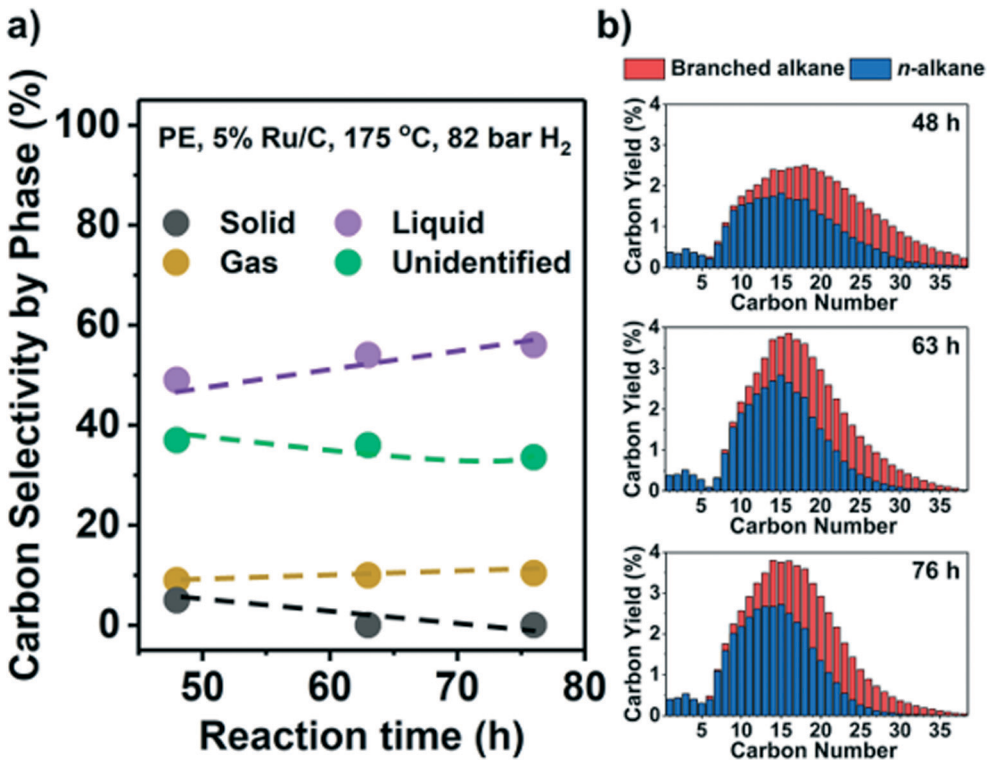

Fig. 5 Hydrogenolysis of PE under optimal conditions (175 °C, 82 bar H_2) for high liquid yield. The C yield of solid (black), liquid (purple), and gas (yellow), along with unidentified C (green), are shown in a). The C distribution in C_1–C_{38} products is presented in b), with gas products plotted at a one-fifth scale. A liquid yield of >57% was achieved.

 This journal is © The Royal Society of Chemistry 2022

Open Access Article. Published on 02 February 2022. Downloaded on 9/2/2025 8:32:14 PM.
This article is licensed under a Creative Commons Attribution-NonCommercial 3.0 Unported Licence.

solid residue fraction increased from 39.0% without PVC, to 67.6% with 0.1 wt% PVC, and further to 93.2% with 1 wt% PVC (175 °C, 30 bar H_2). Control experiments showed that the presence of HCl solution with a Cl content equal to 1 wt% PVC had a similar impact (Table S5†). Therefore, the development of Cl-resistant catalysts or Cl-removal procedures from the feedstock is mandatory. Despite the lower catalytic efficiency, the presence of PVC directs the regioselectivity of hydrogenolysis towards internal C–C bond cleavage and favors branched over linear products (Table S5†). This indicates that Cl at the metal surface particularly hinders the adsorption of ^{3}C (*i.e.*, ^{3}C–^{1}C and ^{3}C–^{2}C cleavage). We characterized the spent catalyst by scanning transmission electron microscopy/energy dispersive X-ray microscopy (STEM/EDX) and by elemental analysis to interrogate the fate of Cl. The signals of Ru and Cl in EDX overlap (Fig. S9b†). Therefore, we could not identify Cl associated with Ru particles. However, we found Cl in areas with few highly disperse Ru particles (Fig. S9c and d†). Thus, we surmise that Cl remains randomly distributed across the used catalyst. According to elemental analysis, a spent sample contains 0.2 wt% Cl, which suggests that 3% of the initial Cl remains in the catalyst. Most of the initial Cl is likely eliminated as HCl, which was detected, but not quantified, after the reaction.

4. Conclusions

The solvent-free hydrogenolysis of polypropylene (PP; $M_W \sim 250\,000$) and polyethylene (PE, $M_W \sim 4000$) using Ru/C catalysts is a low-temperature upcycling approach with high yield to liquid alkanes. Its activity surpasses that of other C-supported Pt-group metals with equal particle size. On Ru/C, C_6–C_{38} alkanes were produced in the temperature range of 175–225 °C from PP and 150–200 °C from PE. PP produces mainly CH_4 and branched hydrocarbons, while PE produces CH_4 and branched and linear alkanes. Increasing H_2 pressure shifts the regioselectivity of hydrogenolysis from terminal C–C towards internal C–C cleavage, thus reducing CH_4 production, and favors linear over branched products. These trends in product distribution result from the interplay between 1) the structure of the polymers, 2) the positions along the chain, where C–C units bind to the metal, and 3) the space available at the metal for the dehydrogenation step prior to C–C cleavage. The CH_4 selectivity and product distribution in liquid and gas do not change significantly with reaction time or conversion of the initial polymer. This is attributed to the favored adsorption of long-chain polymers over shorter alkanes. Instructed by the findings, we achieved >57% yield of C_6–C_{38} alkanes under optimal conditions. This work demonstrated the feasibility of upcycling both PP and PE by hydrogenolysis and identified Ru/C as a more effective catalyst than the commonly studied Pt. The comparative study on the polyolefin structure, temperature, reaction time, and H_2 pressure establishes practical guidelines for improving the product distribution and fundamental knowledge on the reaction mechanism.

Conflicts of interest

The authors declare that they have no known competing financial interests or personal relationships that could have appeared to influence the work reported in this paper.

Acknowledgements

L. C. M., L. V. H., J. A. L., and O. Y. G. were supported by the US Department of Energy (DOE), Office of Science, Office of Basic Energy Sciences (BES), Division of Chemical Sciences, Geosciences and Biosciences (towards a polyolefin-based refinery: understanding and controlling the critical reaction steps, FWP 78459). L. C., T. T. L., A. K., and J. S. were supported by the DOE, Office of Science, BES, Division of Chemical Sciences, Geosciences and Biosciences (impact of catalytically active centers and their environment on rates and thermodynamic states along reaction paths, FWP 47319). We gratefully acknowledge Libor Kovarik for STEM/EDX analysis at Pacific Northwest National Laboratory (PNNL) and Teresa Lemmon and Marie Swita also at PNNL for their help with elemental analysis.

References

1 I. Tiseo, *Annual production of plastics worldwide from 1950 to 2020*, Statista, https://www.statista.com/statistics/282732/global-production-of-plastics-since-1950/, (last accessed Aug, 2021).
2 *How much oil is used to make plastic?*, U.S. Energy Information Administration Website, https://www.eia.gov/tools/faqs/faq.php?id=34&t=6, (last accessed Aug, 2021).
3 *How much oil is used to make plastic?*, Beston Machinery Website, https://plasticpyrolysisplants.com/much-oil-used-make-plastic/, (last accessed Aug, 2021).
4 A. Ghaddar and R. Bousso, *Rising use of plastics to drive oil demand to 2050*, IEA, Reuters Website, https://www.reuters.com/article/us-petrochemicals-iea/rising-use-of-plastics-to-drive-oil-demand-to-2050-iea-idUSKCN1ME2QD, (last accessed Aug, 2021).
5 D. K. A. Barnes, F. Galgani, R. C. Thompson and M. Barlaz, *Philos. Trans. R. Soc., B*, 2009, **364**, 1985–1998.
6 R. Geyer, J. R. Jambeck and K. L. Law, *Sci. Adv.*, 2017, **3**, e1700782.
7 W. Kaminsky, B. Schlesselmann and C. Simon, *J. Anal. Appl. Pyrolysis*, 1995, **32**, 19–27.
8 R. Bagri and P. T. Williams, *J. Anal. Appl. Pyrolysis*, 2002, **63**, 29–41.
9 W. Kaminsky and I.-J. N. Zorriqueta, *J. Anal. Appl. Pyrolysis*, 2007, **79**, 368–374.
10 T. Okui and Y. Ogo, *J. Appl. Polym. Sci.*, 1980, **25**, 747–759.
11 V. Dufaud and J.-M. Basset, *Angew. Chem., Int. Ed.*, 1998, **37**, 806–810.
12 G. Tosin, C. C. Santini and J.-M. Basset, *Top. Catal.*, 2009, **52**, 1203–1210.
13 X. Jia, C. Qin, T. Friedberger, Z. Guan and Z. Huang, *Sci. Adv.*, 2016, **2**, e1501591.
14 G. Celik, R. M. Kennedy, R. A. Hackler, M. Ferrandon, A. Tennakoon, S. Patnaik, A. M. LaPointe, S. C. Ammal, A.

Open Access Article. Published on 02 February 2022. Downloaded on 9/2/2025 8:32:14 PM.
This article is licensed under a Creative Commons Attribution-NonCommercial 3.0 Unported Licence.

Heyden, F. A. Perras, M. Pruski, S. L. Scott, K. R. Poeppelmeier, A. D. Sadow and M. Delferro, *ACS Cent. Sci.*, 2019, **5**, 1795–1803.
15 A. Tennakoon, X. Wu, A. L. Paterson, S. Patnaik, Y. Pei, A. M. LaPointe, S. C. Ammal, R. A. Hackler, A. Heyden, I. I. Slowing, G. W. Coates, M. Delferro, B. Peters, W. Huang, A. D. Sadow and F. A. Perras, *Nat. Catal.*, 2020, **3**, 893–901.
16 F. Zhang, M. Zeng, R. D. Yappert, J. Sun, Y.-H. Lee, A. M. LaPointe, B. Peters, M. M. Abu-Omar and S. L. Scott, *Science*, 2020, **370**, 437–441.
17 L. Yao, J. King, D. Wu, S. S. C. Chuang and Z. Peng, *Catal. Commun.*, 2021, **150**, 106274.
18 S. P. Ertem, C. E. Onuoha, H. Wang, M. A. Hillmyer, T. M. Reineke, T. P. Lodge and F. S. Bates, *Macromolecules*, 2020, **53**, 6043–6055.
19 Y. Jing, Y. Wang, S. Furukawa, J. Xia, C. Sun, M. J. Hülsey, H. Wang, Y. Guo, X. Liu and N. Yan, *Angew. Chem., Int. Ed.*, 2021, **60**, 5527–5535.
20 J. E. Rorrer, G. T. Beckham and Y. Román-Leshkov, *JACS Au*, 2021, **1**, 8–12.
21 C. Jia, S. Xie, W. Zhang, N. N. Intan, J. Sampath, J. Pfaendtner and H. Lin, *Chem Catalysis*, 2021, **1**, 437–455.
22 Y. Nakaji, M. Tamura, S. Miyaoka, S. Kumagai, M. Tanji, Y. Nakagawa, T. Yoshioka and K. Tomishige, *Appl. Catal., A*, 2021, **285**, 119805.
23 P. A. Kots, S. Liu, B. C. Vance, C. Wang, J. D. Sheehan and D. G. Vlachos, *ACS Catal.*, 2021, **11**, 8104–8115.
24 J. E. Rorrer, C. Troyano-Valls, G. T. Beckham and Y. Román-Leshkov, *ACS Sustainable Chem. Eng.*, 2021, **9**, 11661–11666.
25 J. H. Sinfelt, *Catal. Rev.*, 1970, **3**, 175–205.
26 J. H. Sinfelt, in *Advances in Catalysis*, ed. D. D. Eley, H. Pines and P. B. Weisz, Academic Press, 1973, vol. 23, pp. 91–119.
27 J. H. Sinfelt, *Catal. Lett.*, 1991, **9**, 159–171.
28 C. J. Machiels and R. B. Anderson, *J. Catal.*, 1979, **58**, 268–275.
29 H. Shi, O. Y. Gutiérrez, A. Zheng, G. L. Haller and J. A. Lercher, *J. Phys. Chem. C*, 2014, **118**, 20948–20958.
30 H. Shi, O. Y. Gutiérrez, H. Yang, N. D. Browning, G. L. Haller and J. A. Lercher, *ACS Catal.*, 2013, **3**, 328–338.
31 M. D. Boot, M. Tian, E. J. M. Hensen and S. Mani Sarathy, *Prog. Energy Combust. Sci.*, 2017, **60**, 1–25.
32 D. D. Hibbitts, D. W. Flaherty and E. Iglesia, *J. Phys. Chem. C*, 2016, **120**, 8125–8138.
33 D. W. Flaherty and E. Iglesia, *J. Am. Chem. Soc.*, 2013, **135**, 18586–18599.
34 D. W. Flaherty, D. D. Hibbitts and E. Iglesia, *J. Am. Chem. Soc.*, 2014, **136**, 9664–9676.
35 Y. Nakagawa, S.-I. Oya, D. Kanno, Y. Nakaji, M. Tamura and K. Tomishige, *ChemSusChem*, 2017, **10**, 189–198.
36 F. G. Gault, in *Advances in Catalysis*, ed. D. D. Eley, H. Pines and P. B. Weisz, Academic Press, 1981, vol. 30, pp. 1–95.
37 A. Cimino, M. Boudart and H. Taylor, *J. Phys. Chem.*, 1954, **58**, 796–800.
38 G. Maire, G. Plouidy, J. C. Prudhomme and F. G. Gault, *J. Catal.*, 1965, **4**, 556–569.
39 K. Morikawa, W. S. Benedict and H. S. Taylor, *J. Am. Chem. Soc.*, 1936, **58**, 1795–1800.
40 C. Kemball and H. S. Taylor, *J. Am. Chem. Soc.*, 1948, **70**, 345–351.
41 I. Chorkendorff and J. W. Niemantsverdriet, *Concepts of modern catalysis and kinetics*, John Wiley & Sons, New York, 2007.
42 J. Kua, F. Faglioni and W. A. Goddard, *J. Am. Chem. Soc.*, 2000, **122**, 2309–2321.
43 H. Shi, O. Y. Gutiérrez, G. L. Haller, D. Mei, R. Rousseau and J. A. Lercher, *J. Catal.*, 2013, **297**, 70–78.
44 Z. Zhou, S. Pesek, J. Klosin, M. S. Rosen, S. Mukhopadhyay, R. Cong, D. Baugh, B. Winniford, H. Brown and K. Xu, *Macromolecules*, 2018, **51**, 8443–8454.
45 E. Nordmeier, U. Lanver and M. D. Lechner, *Macromolecules*, 1990, **23**, 1072–1076.
46 M. Jung, Y. Lee, S. Kwak, H. Park, B. Kim, S. Kim, K. H. Lee, H. S. Cho and K. Y. Hwang, *Anal. Chem.*, 2016, **88**, 1516–1520.

This journal is © The Royal Society of Chemistry 2022